Polymer Surfaces, Interfaces and Thin Films

Manfred Stamm
Max Planck-Institut für Polymerforschung
Postfach 3148, 55021 Mainz, Germany

ABSTRACT

Neutron reflectometry can be used in various ways to investigate surfaces, interfaces and thin films of polymers. Its potential comes mostly from the possibilities offered by selective deuteration, where a particular component can be made visible with respect to its activity at the interface. In addition the depth resolution is much better than with most other direct techniques, and details of the profiles may be resolved. Several examples will be discussed including the segment diffusion at the interface between two polymer films, the determination of the narrow interfaces between incompatible polymer blends and the development of order in thin diblock copolymer films.

1. Introduction

Neutron reflectivity techniques are used in various areas of polymer science for the investigation of polymer surfaces, interfaces and thin films. This includes interdiffusion, blending, roughening, development of surface induced order, adsorption or surface enrichment of components. Several excellent reviews of different aspects in this area have been published (see e.g. reviews by Russell [1,2], Stamm and Schubert [3,4], Richards and Penfold [5] and Foster [6]). In those studies quite often the particular surface and interface properties are in the focus, but it is also tried in many cases to use the thin films as model systems for the determination of properties and parameters of the bulk state, which otherwise cannot easily be obtained. An example in both respects are polymer blend systems, where the surface induced ordering of diblock copolymers is a typical surface phenomena, while the segment diffusion across the interface of two polymer films and the determination of the interface width in incompatible polymer blends is used to draw conclusion on segment mobility and blend compatibility also for the bulk state.

We will use polymer blends and copolymers also here as examples to demonstrate the possibilities of the neutron reflectivity technique. Polymer blends and copolymers are used in an increasing area of applications, since they offer a cost effective way and a large potential to design optimized materials with properties tailored to quite a specific use. Thus polymer blends, composites and light-weight reinforced polymer materials are utilized for instance in various parts of cars or airplanes with different demands on material properties, which in addition also differ from manufacturer to manufacturer. The materials industry has to meet those demands for an increasing spectrum of applications, which is impossible to do through the development of chemically completely new polymers. Therefore existing materials are tried to be modified or blended, and the understanding of microstructures and polymer-polymer interactions gains increasing importance.

For this reason the question of polymer miscibility is attributed great importance [7,8]. Most polymers turn out to be incompatible with each other. They form microphase separated structures, when they are mixed together. To obtain good mechanical properties good cohesion between phases is required, and different materials have to interpenetrate with each

other at the interface [9,10]. This interpenetration depends on the degree of miscibility of components and is generally neither easy to determine experimentally nor easy to predict theoretically. For most incompatible materials, the interface is not very wide and typically in the range of 1 to 20 nm, depending on compatibility. This can be nicely measure by neutron reflectometry in a multilayer set-up as shown in Fig. 1. If two incompatible polymers in the melt are put into contact, some interpenetration will occur. The interface width increases with time reaching an equilibrium value, which according to mean field theory is determined by the segment interaction parameter χ. From a more detailed and systematic knowledge of the interface parameters (for instance the interface width σ in Fig.1) for different polymeric materials, one could expect to obtain a better understanding of polymer miscibility.

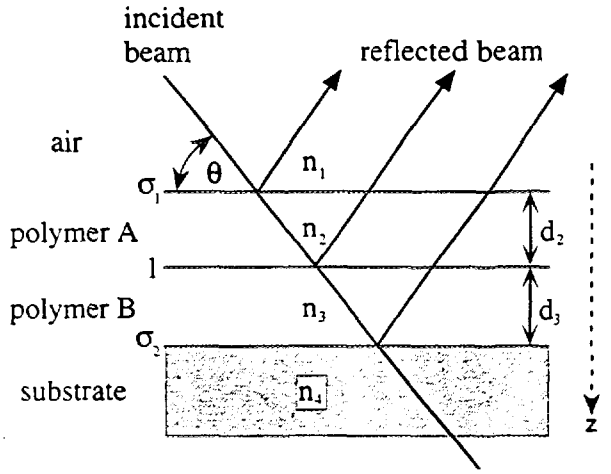

Fig.1 Schematics of a neutron reflectivity experiment from two polymer films deposited on a substrate. Parameters indicated are film thicknesses d_i, indices of refraction n_i, interface widths σ_i and the angles of the incident and transmitted beam θ_i, respectively.

Besides equilibrium thermodynamic effects, other factors originating from sample preparation and experimental conditions also influence interface formation. Putting two films together, this includes the influence of initial surface roughness, surface composition and chain conformation at the surface of the films, which may largely depend on sample history. In specific cases it will be difficult to reach equilibrium, for instance when segment mobility is slow due to the vicinity of the glass transition T_g. It will generally be interesting to follow the time dependence of interface formation. Since the width for incompatible polymers is typically smaller than 20 nm, the resolution of techniques has to be adopted for a determination of interface width and profile [11,12,13]. Besides resolution requirements, a suitable contrast between components has to be present to be able to "see" the interface between the components. This contrast can be generated for neutron reflectometry, for example, by the suitable deuteration of one component. Neutron reflectometry is thus of quite general use, and also in multicomponent systems one component and its interfaces with other components can be made "visible" for neutrons. It is, however, in any case advisable to use other complementary surface and interface analysis techniques [11,12,13] including ellipsometry, x-ray reflectometry, interference microscopy, ion beam techniques, interface tension, electron microscopy or atomic force microscopy, which provide in many cases information, which cannot be obtained by neutron reflectivity alone and which helps considerably in the interpretation of the neutron results.

Since the technique of neutron reflectivity has already been introduced by the previous contributions, we will in the following only describe some specific aspects of polymers including contrast problems, sample preparation, and some instrumental details. Then we will

try to emphasize some of the advantages of neutron reflectometry as compared to the other most common techniques for the investigation of polymer surfaces and interfaces, and also will discuss some of the problems connected with this technique. We then will present some examples of polymer surfaces, interfaces and thin films demonstrating the possibilities and the potential of the technique in the area of polymer science.

2. General aspects for the application of neutron reflectometry to polymers

2.1 The contrast between components

Neutron reflectometry is a very versatile technique to investigate accurately interfacial aspects and thin films of polymers [1-6] since a contrast between components can in most cases be achieved by the deuteration of one component. It then provides a depth resolution typically of the order of 0.2 nm. The technique can be applied to practically all polymeric systems, provided one component can be deuterated. This might, however, require a significant effort from the chemical preparation side. Analogous to optics, one can specify a refractive index for neutrons :

$$n = 1 - (\lambda^2/2\pi)\, b\, \rho_n - i\,(\lambda/4\pi)\, \mu_n \qquad (1)$$

$b\rho_n$ is the neutron scattering length density (b is the scattering length, ρ_n the particle number density), μ_n the linear absorption coefficient for neutrons, and λ the wavelength. The interaction between matter and neutrons is generally weak, and the refractive index n is very close to 1 (i.e. $n \sim 1\text{-}10^{-6}$). For neutrons true absorption is in most cases negligible. One may compare the situation to x-ray reflectometry, where the index of refraction is similarly given by an expression like equ.(1), but where $b\ \rho_n$ has to be replaced by $a_e\ \rho_e$. Here a_e and ρ_e now represent the classical electron radius and the electron density, respectively. To illuminate the contrast problem, the scattering densities for neutrons and x-rays for some materials are compiled in table 1. It is evident from a comparison of the deuterated and protonated materials that a large contrast can be obtained for neutrons by deuteration. In the case of x-rays, contrasts even for significantly different polymers are not large, and a typical situation is depicted in Fig. 2. Thus, X-ray experiments are only possible for the investigation of some particular polymer systems with large differences in the electron density, but neutron reflectometry proves to be a much more versatile technique due to the possibility to generate a huge contrast between components by deuteration. It should of course be kept in mind that deuteration also changes thermodynamics slightly, which, however, for many systems can be neglected.

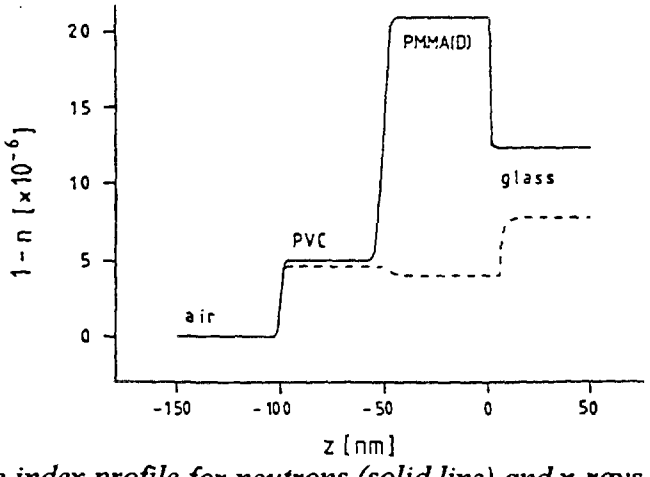

Fig. 2 Refractive index profile for neutrons (solid line) and x-rays (dashed line) of a layer system of PMMA and PVC on float glass

Compounds	chemical formulas	ρ [g cm^{-3}]	$a_e\rho_e$ [10^{10} cm^{-2}]	$b\rho_n$(H/D) [10^{10} cm^{-2}]	μ_x [cm^{-1}]	μ_n(H/D) [cm^{-1}]
air/vacuum		0	0	0	0	0
PS	$(C_8H_8)_n$	1.03	9.5	1.41/6.46	4	3.9/0.6
PMMA	$(C_5H_8O_2)_n$	1.15	10.6	1.06/7.02	7	4.5/0.6
PVC	$(C_2H_3Cl)_n$	1.38	12.1	1.56/5.76	86	3.3/0.5
PBrS	$(C_8H_7Br)_n$	1.57	13.2	1.76/5.58	97	4.0/0.6
quartz	SiO_2	2.3	19.7	4.20	85	0.2
silicon	Si	2.33	19.7	2.15	141	0.1
nickel	Ni(^{58}Ni)	8.91	72.6	9.25 (12.9)	407	2.6
gold	Au	19.32	131.5	4.48	4170	3.3

Table 1. Characteristic data for the reflection of x-rays and neutrons at interfaces: mass density ρ_n, electron scattering densities $a_e\rho_e$, neutron scattering length densities $b\rho_n$(H/D) for protonated (H) / deuterated (D) compounds, and linear absorption coefficients for X-rays and neutrons, μ_x (at a wavelength λ= 0.154 nm) and μ_n (at λ= 0.1 nm), respectively. The two values in some of the columns correspond to the H- and D- materials, respectively.

2.2 Sample preparation

Neutron reflectometry needs, however, a dedicated sample preparation, where relatively large (typically 5 x 10 cm^2) thin films have for instance to be deposited on top of each other. Interfacial roughness (typically 1 nm or larger) also limits in some cases the resolution. A typical sample geometry is shown in Fig.1. A thin film of polymer A has been deposited by the floatation technique on top of a film of polymer B. Typical film thicknesses are in the range from 10 to 300nm, and to achieve a reasonable smoothness and surface roughness, spin coating techniques for the preparation of single films are used. A second film is mechanically deposited on another one by floating it off in a bath of water and picking it up with another film on a substrate. In this way even multilayer samples may be produced. Since both films are solid at room temperature, no interdiffusion takes place at the interface, but can be initiated by heating later. Water is removed by heating to a temperature below T_g under vacuum. Suitable substrates for film deposition are for instance float glass, silicon wafers or generally polished flat surfaces. Since the determination of a reflection curve takes between 2 to 12 h, samples are mostly annealed outside the reflectometer and then quenched for the neutron experiments below the glass transition temperatures of the materials. Because of the slow interdiffusion process of segments at the interface, samples sometimes have to be annealed for several days before the equilibrium interface width is achieved.

2.3 Instrumentation

There are generally two types of instruments existing described already before: single wavelength or time-of-flight reflectometers. The instrument TOREMA II at Geesthacht for instance utilizes a graphite monochromator and is operated at a fixed wavelength of 0.43nm (similar to [14]). In a reflectivity scan the sample is rotated and the reflected intensity recorded on the linear detector. In Geesthacht we are, however, presently constructing a new reflectometer PNR [15] at the end position of a neutron guide, which combines some of the elements of both set-ups (Fig.3). It utilizes a velocity selector, which allows in combination with a chopper the selection of a quite variable wavelength distribution (1 to 10%). Accordingly the intensity is significantly increased. The instrument may be operated in three different modes: (i) at fixed wavelength rotating the sample, (ii) at variable wavelength changing the wavelength with the velocity selector, or (iii) in TOF mode utilizing the chopper.

There are also polarization facilities and an area detector to also determine off-specular intensity.

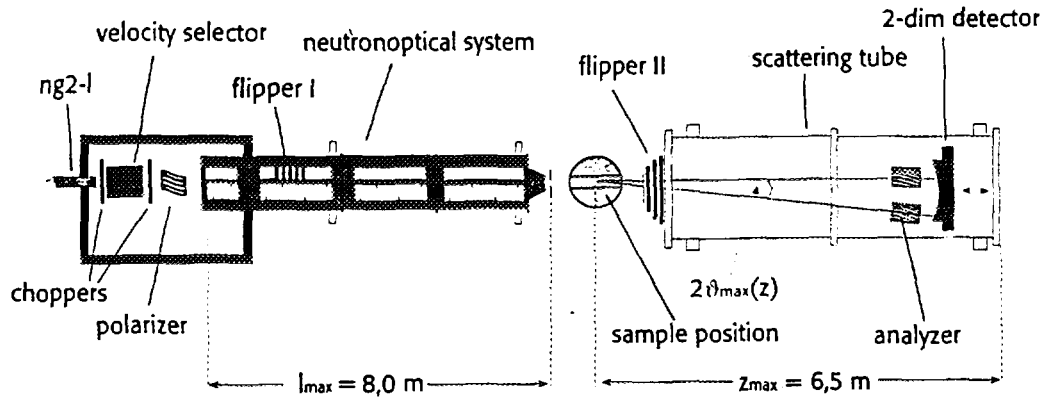

Fig.3 Schematics of the polarized neutron reflectometer PNR at Geesthacht presently under construction.

2.4 Data analysis

The reflectivity as a function of the angle of incidence can be calculated from the refractive index profile using a matrix formalism [16]. Relevant parameters are indicated in Fig.1. Error functions characterized by their variances σ_1^2 and σ_2^2, respectively, are usually employed to describe the roughnesses of the interfaces air / polymer A and polymer B / substrate. A tanh-refractive index profile with the characteristic parameter l (see equ. (6a)) is commonly used between polymer A and B. Finally, the thicknesses d_2 and d_3, and the refractive indices n_1 to n_4 are parameters for a fit, which, however, can be determined by separate measurements prior to the experiment for the determination of the interface width l. There are also techniques described for a model free fitting (see e.g. references in [4]). It is important to note that (specular) reflectivity techniques do not provide lateral information and reflection curves are averaged laterally over the sample (lateral coherence length is typically several micrometers). There is in principle the possibility to obtain lateral information from off–specular scans, which, however, in most experiments is not done for intensity reasons. Non-uniqueness of data analysis, which might be a problem in some more complicated cases of the application of the technique, is mostly not a problem for the analysis of a double layer system, since the starting situation is very well defined.

2.5 Advantages and limitations of the technique

There are several advantages of neutron reflectometry over other common interface analysis techniques. First the generation of the contrast by deuteration offers various possibilities. Thus for the same system also different contrasts may be chosen to reveal different aspects of the structure. Second the depth resolution of typically 0.2nm is very good as compared to most other techniques. Thus also very thin interfaces can be still resolved and the resolution is mostly limited by the quality of the sample preparation. Third also hidden interfaces well within the material may be investigated. As an example neutrons can easily penetrate 10cm of a silicon crystal to determine the interface between this crystal and a polymer in solution. Experiments under external fields (pressure, shear etc.) are therefore not so difficult. Finally the technique provides information also about various details of the shape of profile. This can be taken as an advantage, but in some cases may also turn out as a

disadvantage, since the interesting aspect may be hidden behind some other unexpected changes.

One thus might also note some of the disadvantages. The need of detailed model fits for the determination of parameters is certainly one of the main disadvantages. Those fit are usually not unique, and in some cases it turns out to be very time consuming to obtain reasonable fits. It is thus very helpful to obtain additional data on film thicknesses, roughnesses, surface enrichment of components etc. from other more direct techniques even if the resolution is much worse. Secondly the profile is averaged laterally, and it is very difficult to obtain information on lateral structures from neutron reflectivity alone. Here also other complementary techniques should be used. The large illuminated sample area thirdly poses severe requirements on the quality of the sample preparation, since samples have to be smooth on a nanometer-scale over several centimeters to achieve good depth resolution.

For a given problem it is thus very advisable to "compose" the sample already well in advance based on model calculations. One should try to obtain as much as possible additional information from complementary techniques, and it is hardly possible to obtain reliable results from multilayer systems or structured films without further knowledge about the sample.

3. Interfaces between incompatible polymers

As an example for the neutron reflectivity technique, where the good resolution together with a high contrast at the interface is needed, we will consider in some detail the formation of the narrow interfaces between incompatible polymers. In spite of the widespread use and application of incompatible polymer blends, only a limited number of experimental studies has been reported in literature. This is probably due to the fact that the narrow interface widths are hard to determine experimentally. Values reported from different techniques are then also not always compatible with each other and are scattered over quite a range. We will discuss some of the more recent investigations in more detail, where effect of compatibility, glass transition and temperature on interface width has been studied for several systems. A comparison of some data is given in table 2.

3.1 Theoretical aspects

For the description of phase behavior in polymer blends in a first approach the Flory, Huggins and Staverman (FHS) theory is used (for a review see e.g. [17]). With a lattice model a simple form for the free energy F_{FHS} of binary polymer blends including the segment interaction parameter χ is derived

$$\frac{F_{FHS}}{kT} = \frac{\phi \ln \phi}{N_1} + \frac{(1-\phi)\ln(1-\phi)}{N_2} + \chi\phi(1-\phi) \qquad (2)$$

N_1 and N_2 are the degrees of polymerization, T is the temperature and ϕ is the concentration of one component. To discuss the problem of an interface between two polymers, equation (2) has to be extended by the so-called square gradient term $\kappa(\nabla\phi)^2$ introduced by Cahn and Hilliard [18] to take fluctuations into account. Due to different approximations there are different prefactors. A discussion of the prefactor is for instance also given in [19]. For the case, where structures are in the range of the radii of gyration (R_g) of components or smaller ($qR_g>1$), one obtains a particular prefactor for the interface width $a_I = 2l$. An exact analytical solution for the volume fraction profile ϕ can be calculated for the case of infinite degrees of polymerization ($\chi N>>1$) using Euler-Langrange equation.

$$\phi(z) = \frac{1}{2}\left(1+\tanh\frac{z}{l}\right) \qquad (3)$$

where z is a coordinate across the interface and l is given by

$$l = \frac{a}{\sqrt{6\chi}} \tag{4}$$

a is the mean segment length of the components. For structures which are large compared to the radii of gyration ($qR_g << 1$) a different prefactor is derived

$$l = \frac{a}{\sqrt{9\chi}} \tag{5}$$

The influence of finite chain length on interface formation has been considered by several authors (for a review see e.g. [4, 17]). Three different methods yield slightly different expressions for the interface width l with finite chain length. Brosetta [20] derives the expression

$$l = \frac{a}{\sqrt{6\left(\chi - 2\ln 2\left(\frac{1}{N_1} + \frac{1}{N_2}\right)\right)}} \tag{6}$$

The fundamental result of the square gradient theory applied to the description of the interface between incompatible polymers is the direct connection of the interfacial width with the interaction parameter χ.

$$l \propto \chi^{-0.5} \tag{7}$$

In particular, computer simulations allow the incorporation of interactions and dynamics in a quite versatile way [21] and reveal asymmetry effects as well as the influence of fluctuations or capillary waves, which are mostly not included in analytic treatments. The analysis of experimental data on the basis of equ. (4) - (7) still has to be performed with care, since most experimental techniques measure an "apparent" interface width, which, due to lateral averaging, also contains the influence of lateral inhomogeneities, initial interfacial roughness due to preparation conditions and capillary waves or compositional fluctuations. Also not included in most theoretical treatments is the specific effect of chain ends, which may be enriched at the interface and which in general are of a different chemical nature as the rest of the chains including for instance some groups from the catalyst. The presence of a broad molecular weight distribution will also result in a broadening of the interface, in particular, if low molecular weight components are present. This effect can be estimated on the basis of equ. (6) and may lead to a fractionation of components at the interface.

3.2 Interfaces between Polystyrene(PS)/Polymethylmethacrylate (PMMA)

One of the most intensively studied incompatible blend systems is PS/PMMA. We have prepared a sample of a deuterated PS film (M_W=720k) on top of a protonated PMMA (M_W=35k) film by the floatation technique [22]. Both films were prepared by spin-coating from toluene solution. Substrates are float glass plates with a typical surface roughness of 1nm. Neutron reflectivity experiments have been performed at TOREMA II in Geesthacht. The reflectivity curves are shown in Fig. 4 before and after annealing for 24h at 140°C. Changes are observed in particular at large k_z corresponding to small interdiffusion distances. Also shown in Fig. 4 are the fit curves, which provide the interface widths. It changes from a_I^0 = 3.0nm for the unannealed to a_I^e = 4.6nm for the annealed sample. Also shown is a fit for the annealed sample assuming the interface width of the unannealed sample for the fit (Fig.4c). This demonstrates the accuracy of the technique for the determination of the interface width, which is of the order of 0.4nm in this case. For the determination of the interdiffusion distance of the two materials one has to take the difference between the final and initial value,

$$a_I = \sqrt{(a_I^e)^2 - (a_I^0)^2} \quad . \tag{8}$$

The use of this equation assumes that the initial interfacial roughness does not change during annealing and that the two effects, interdiffusion and roughness, can be superposed. We similarly have performed experiments with PMMA materials of different molecular weights, showing the increase in interface width with decreasing molecular weight. The results are summarized in Fig.5. Also shown in Fig.5 is a fit curve based on equ.(6). From such a fit on the molecular weight dependence of the interface width one can obtain the two relevant parameters in equ.(6), the segment interaction parameter χ = 0.0326 (± 0.0058) and the segment length a = 0.73 (±0.13)nm. From the measurement of interface parameters one thus can learn something about important thermodynamic quantities of this blend system. The segment interaction parameters for incompatible blend systems are not easy to obtain otherwise.

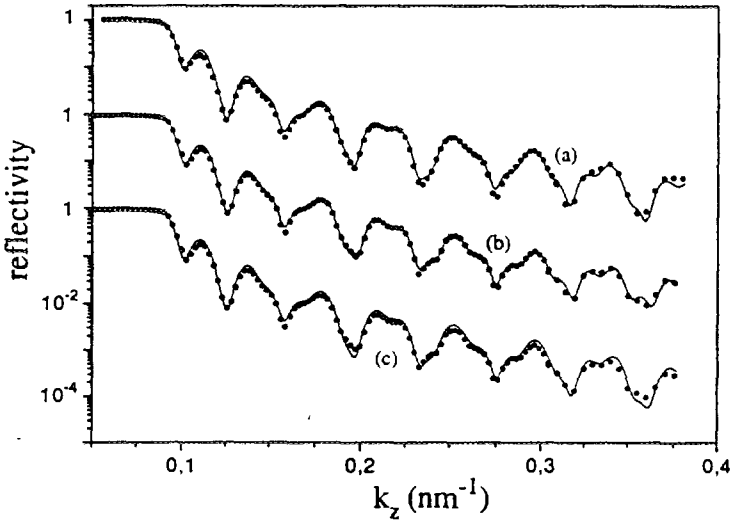

Fig.4 Neutron reflectivity data and fits (solid lines) before (a) and after (b) annealing of a PS(D)/PMMA(H) double film system on a glass plate. The fit of curve (c) is performed with the interface width of the unannealed sample.

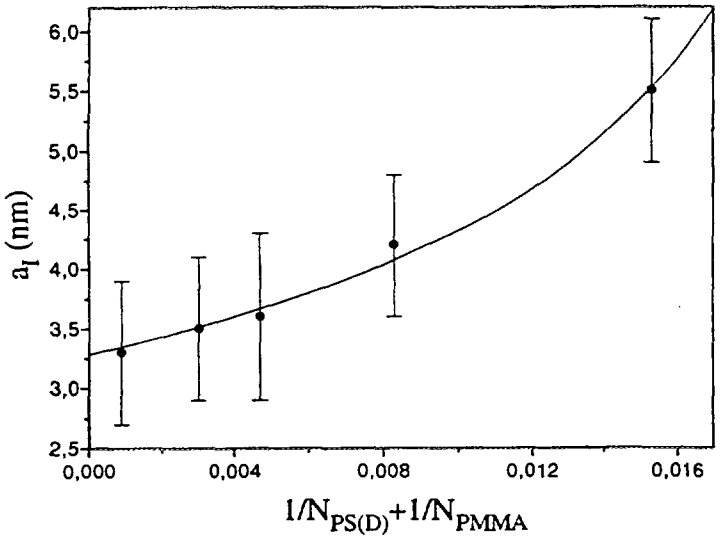

Fig.5 Interface width of PS(D)/PMMA(H) as a function of the degree of polymerization. The solid line corresponds to a fit according to equ.(6) as explained in the text.

For comparison values of interface widths $a_I = 2l$ determined with different techniques are compiled in table 2. One of the most accurate values has been obtained by Anastasiadis et al. [23] with neutron reflectometry. It has been confirmed from other NR-studies of those authors with diblock copolymers, where also this interface width between lamellae is found to

be of the same size. The value of a_I = 5.0nm is also consistent with NR data of Fernandez et al. [23] after suitable recalculation of their original values. Both values are higher than the ones measured by us, but have not been corrected for initial roughness according to equ.(6). They can be expected to agree within error bars after the correction. Also, temperature dependent ellipsometry investigations [25] and transmission electron microscopy [26] yield similar results within error bars. Elastic recoil detection [27] on the other hand has to be taken with care, since, first, the profile is convoluted by the resolution function, which actually has a width of typically 12 nm and is thus much larger than the investigated interface width, and second, the oxygen profile is recorded, which might be influenced by contaminations of e.g. water at the interface.

Quite low values of the interface width are obtained when the interface width is calculated from interfacial tension data [19,28]. Those interface widths are approximately a factor of 2 smaller than the measured ones before correction for the initial roughness. End-group effects, capillary waves or surface contaminations on the other hand are usually not included in the theoretical treatments. End corrections and concentration fluctuation effects are considered in a recent calculation of Semenov [29], where he concludes that thermal fluctuations of the concentration at the interface can contribute as much as 2 nm to the interface width. In this approximation the coherence length of the reflection experiment enters, and results thus depend on experimental conditions. The agreement is good with a calculated interface width value obtained from a temperature dependent χ-value from SANS-experiments of diblock copolymers [30] on the basis of equ.(6).

Thus the neutron data are consistent with each other, if they are analyzed in a consistent way. They are also consistent with interfacial tension data, which can be taken as a proof of mean field theoretical concepts. Capillary waves and lateral fluctuations seem not to play an important role in the experiments or are already contained in the correction by equ.(6).

	a_i (nm)	T (°C)	$M_r(1)$ (10^3 g mol^{-1})	$M_r(2)$ (10^3 g mol^{-1})	Technique	Comments
PS/PMMA	5±1	170	220	19	NR	—
	5.0±0.5	170	110	107	NR	—
	3–9±1	140–170	180	151	ELLI	—
	5±3	140	180	151	TEM	—
	8	140	180	151	ERD	Error not specified
	(2.6)	190	2–200	24	IT	Calculated from γ_∞
	(2.4)	199	2–43	10	IT	Calculated from γ_∞
	(4.9)	—	110	107	IT	Calculated from γ_∞ with fluctuation and end corrections
	(5.8)	150	13	14	SANS	Calculated from $\chi(T)$ of diblockcopolymer
PS/PBr$_x$S	4.3–9.6±0.6	120–145	160	160	NR	Degree of bromination x = 0.16–1.0
	3.9–6.7±0.6	142	100–1450	100–1450	NR, XR	x = 0.84–0.97
	3.5–4.9±0.4	114–144	117	47	XR	x = 1.0

Tab.2 Interface widths of incompatible polymer systems determined by different techniques[4]

2.3 PS/poly(styrene-stat-para bromo styrene) (PBr$_x$S)

The blend system of PS and the statistical copolymer poly(styrene-stat-para bromo styrene) was chosen for systematic investigations of the dependence of interface width on

compatibility, since the compatibility between components can be easily tuned from completely compatible to highly incompatible by a change in the degree of bromination x. The molecular weight distribution of both partners is narrow. A systematic study of the change of the interface width with the degree of bromination has been performed by neutron reflectometry [31] and results are shown in Fig.6. A low x the interface width diverges, since the system becomes compatible. The functional form is fitted by a composition dependent χ-parameter, which contains the concentration-weighted individual segment-segment interaction parameters of components. Values at large x can be compared to other X-ray and neutron reflectivity data, as shown in table 2. The a_I-values quoted there are, for a better comparison, the ones which have not been corrected for initial surface roughness. There is a very good agreement between different data sets, if high molecular weight data are taken. Some of the differences between different data sets might be due to different temperatures, molecular weights, weight distributions and sample preparations. With some samples also the time dependence of the formation of an equilibrium interface has been followed [31], which is consistent with an initial $t^{0.25}$-behavior and which then levels off to a constant value. In a compatible blend of PS/PBr_xS at low degree of bromination it has been shown by NR [32] that PS migrates to the interface. The form of the profile is consistent with an exponential decay. This system thus can serve as a nice model system with tunable compatibility and variable interface width.

4. Interdiffusion at the interface between compatible polymers

The interdiffusion between compatible polymers can proceed freely over large distances. Most interesting is, however, the segmental movement at early stages of interdiffusion. This can provide general information on the movement of segments of polymers in the melt, where for instance different time scales are discussed in the context of the reptation model. On the other hand this regime has very practical implications in the area of adhesion and welding, since the correlation between segment interdiffusion and mechanical strength at the interface is presently not very well understood. One might distinguish the "selfdiffusion" of a polymer into its deuterated analog versus the interdiffusion of one polymer into another compatible one. We will discuss mostly two cases, the already classical case of the diffusion of PS(H)/PS(D) as well as the interdiffusion of PMMA/PVC, where also the different chain mobilities play a dominant role.

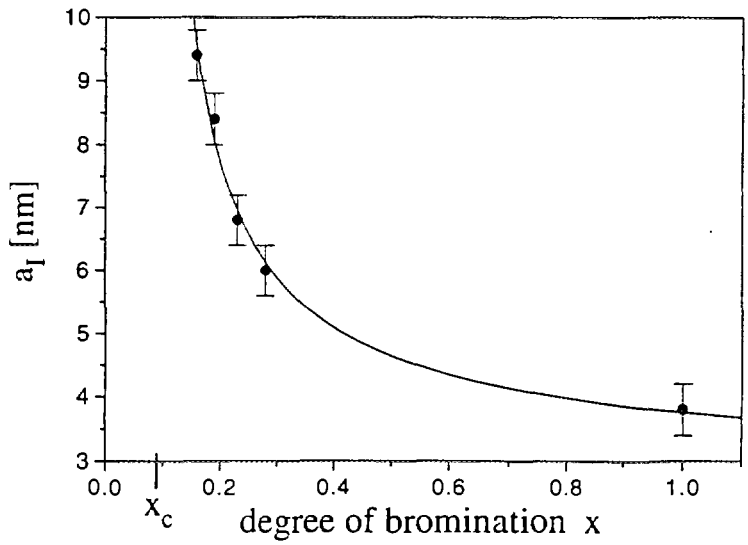

Fig.6 Interface width as a function of the degree of bromination for the system PS(D)/ $PBr_xS(H)$ [31]. The solid line represents a fit according to theory.

4.1 Initial stages of segment diffusion at the interface

The interdiffusion of polystyrenes has been studied by several groups utilizing NR (for reviews see [1,2,3,5,6]). Again a deuterated PS-film is floated on a protonated one, and the broadening of the interface is followed by NR during a sequence of annealing procedures, where the sample is heated above the glass transition temperature (approx. 100°C) for a limited period of time, quenched to room temperature and investigated there. Thus with one sample the time evolution of the interface width can be studied. A typical example is given in Fig.7, where the interface width is plotted versus the annealing time [33]. Clearly different regimes can be distinguished, which are consistent with the reptation predictions. According to the reptation model the diffusion of a chain in the melt is restricted by the entanglements with its neighboring chains. Different time regimes of segmental movement are predicted corresponding first to the movement in a virtual tube formed by the obstacles of the neighboring chains, while at later times the chain can reptate out of the tube. This behavior is nearly quantitatively observed for the movement of segments across the interface. One might on the other hand expect deviations from this ideal behavior due to distorted chain conformations at the interface, chain end effects etc. [3]. Those investigations are thus in strong support of the reptation picture, while the correlation with mechanical properties like adhesion is still not very well established.

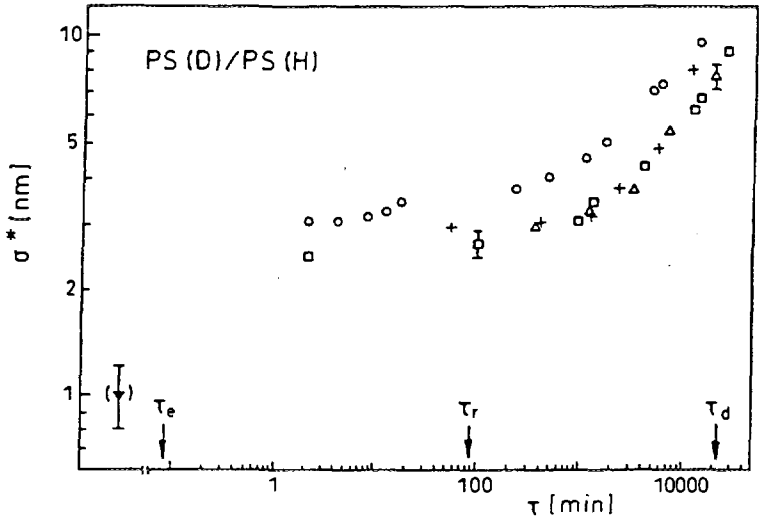

Fig. 7 Interfacial broadening as a function of annealing time for the system PS(D)/PS(H) [33]. The solid lines are guides to the eye. Typical times of the reptation picture are also indicated.

4.2 Influence of chain mobility on segment diffusion

For the case of the miscible blend system PMMA/PVC the mobilities of components are quite different due to different glass transition temperatures (116 and 75°C, respectively). Performing the interdiffusion experiment at a temperature of 114°C for instance, the PMMA material is still in its glassy state and cannot move. However, in a neutron reflectivity experiment (see Fig.8) from a double layer system the dissolution of the immobile PMMA, being below its glass transition at the utilized temperatures, in the mobile component of PVC is observed [34]. This may be explained by a swelling and penetration of the PVC into the PMMA at the interface, leading to a dissolution. Correspondingly the interface moves into the direction of the PMMA film. Already at quite low concentrations of PMMA in PVC on the other hand the diffusion of PMMA to the surface is observed, resulting in a surface enriched layer of PMMA [35]. This is also seen in Fig.8 at later diffusion times and can be confirmed by surface sensitive techniques like XPS or SSIMS.

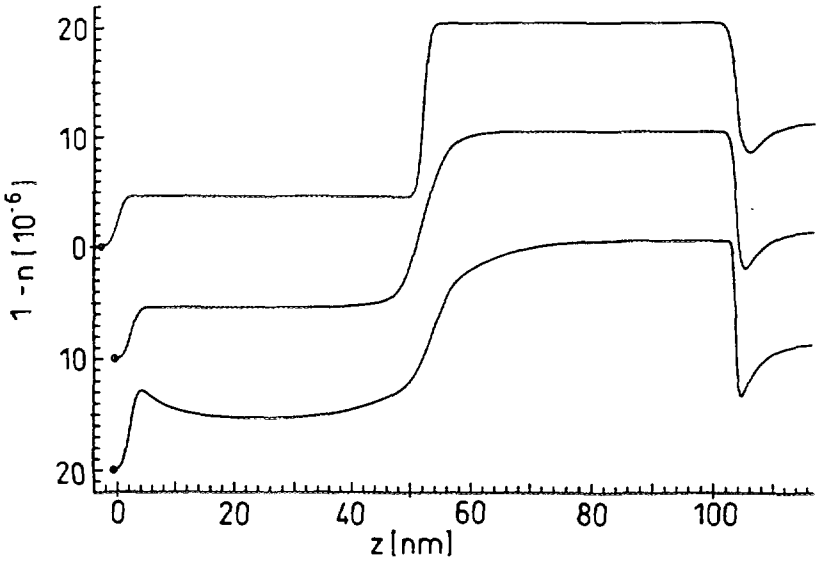

Fig.8 Refractive index profiles obtained from fits to neutron reflectivity curves at different times of annealing for the system PMMA(D)/PVC(H)[34].

5. Order in blockcopolymer thin films

In thin films of diblock copolymers the order induced by the interaction of the different blocks with the surface and substrate has been studied. This leads to a macroscopic ordering of the copolymer in the lamellar phase parallel to the surface. But also in the disordered phase there remains still some order in the vicinity of the surface, which decays with increasing distance.

A system well studied by NR is PS-b-PMMA, where in particular Tom Russell and coworkers have performed very extensive investigations (see reviews [1,2]). Thus it is shown [36] that a thin film in the ordered lamellar phase reveals a multilayered morphology parallel to the surface (Fig.9). The regular arrangement over large distances gives rise to Bragg peaks, while the Kiessig fringes are not resolved due to the large thickness of the film.

When a low molecular weight copolymer is heated into the disordered phase, the lamellar order in the film disappears, while some surface induced order close to the surface and substrate is retained (Fig.10). In subsequent investigations [37] it is shown that the profile at

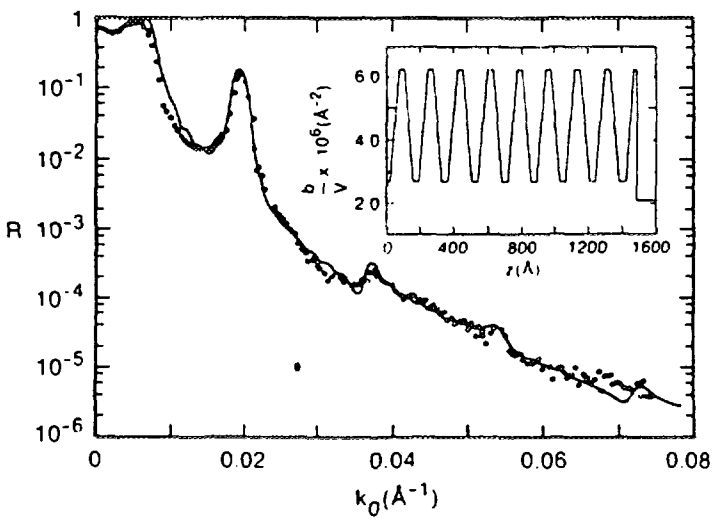

Fig.9 Neutron reflectivity curve and corresponding scattering length density profile (insert) of a thin diblock copolymer film of PS-b-PMMA annealed at 170°C for 24h (from [36]). The solid line corresponds to the fit with the shown profile.

the interface between the lamellae is best described by a hyperbolic tangent function, and that the width of the interface is 5nm. Thus there is no difference observed between the copolymers and the corresponding homopolymers. With very thin films the confined geometry gives rise to changes in the order. It also causes a change in the order-disorder transition temperature [38], which is increasing with decreasing film thickness.

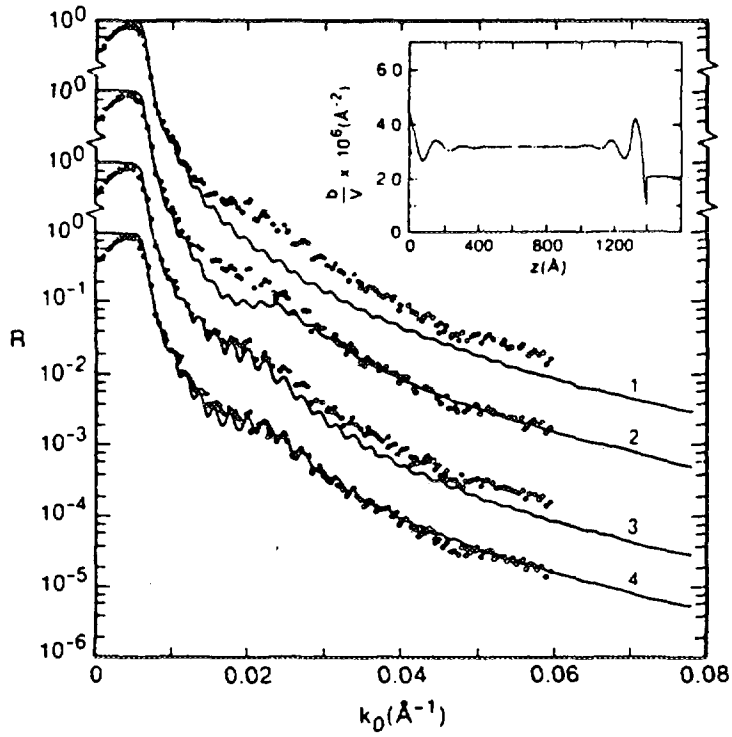

Fig.10 Neutron reflectivity curves of a thin PS-b-PMMA film in the disordered phase (from [36]). For comparison also fit curves with different model profiles are indicated: 1- uniform scattering length density, 2- exponentially damped cosine at the air interface, 3- at the substrate interface, and 4- from both interfaces. The curves have been offset by a factor of 10, respectively.

6. Conclusions

Several examples of the application of neutron reflectivity for the investigation of polymer surfaces, interfaces and thin films have shown the potential of this technique in this area. Several other examples e.g. from the area of polymer adsorption from dilute solution to a solid wall, on the interfacial enrichment of copolymers in homopolymer films or the surface directed spinodal decomposition of polymer blends have not been treated. The technique, however, has been firmly established in the area of polymer science, and can provide information, which is otherwise hardly available.

Acknowledgments
I greatly acknowledge the contributions of Dr. B. Guckenbiehl, Dr. K. Kunz, Dr. D.W. Schubert and Dr. C. Bittorf to this work. Part of this work was supported by BMBF within grant 03-ST4MP2-1.

6. References

1. Russell, T.P., 1990. Mater. Sci. Reports 5: 171
2. Russell, T.P., 1991. Annual Review Materials Sci. 21: 249
3. Stamm, M., 1992. In: *Physics of Polymer Surfaces and Interfaces*. ed. I.C. Sanchez. Boston. Butterworth-Heinemann. 163
4. Stamm, M., Schubert, D.W., 1995. Annual Review Materials Sci. 25: 325
5. Richards, R.W., Penfold, J., 1994. Trends in Pol. Sci. 2: 5
6. Foster, M.D., 1993. Crit. Rev. Analyt. Chem. 24: 179
7. Olabisi, O., Robeson, L.M., Shaw, M.T., 1979. *Polymer-Polymer Miscibility*. New York. Academic Press. 370pp.
8. Utracki, L., 1989. *Polymer Alloys and Blends*. München. Hauser Publishers. 356pp.
9. Kausch, H.H., 1987. *Polymer Fracture*. Heidelberg. Springer Verlag
10. Brown, H.R., Ann. Rev. Mater. Sci. 21: 463
11. Stamm, M., 1992. Adv. in Pol. Sci. 100: 357
12. Tirrell, M., Parsonage, E.E., 1993. *Mater. Sci. and Techn.*, VCH, Weinheim, 12: 653
13. Allara, D.L., Zhang, P., 1994. Mater. Sci. and Techn., Vol. 2BII,VCH, Weinheim, 657
14. Stamm, M., Hüttenbach, S., Reiter, G., 1991. Physica B 173: 11
15. Bittorf, C., Stamm, M., Kampmann, R., Physica B, to be published
16. Lekner, J., 1987. *Theory of Reflection*, Martinus Nijhoff, Dordrecht
17. Binder, K., 1994. Advances in Pol. Sci. 112: 181
18. Cahn, J.W., Hilliard, J.E., 1958. J. Chem. Phys. 28: 258
19. Anastasiadis, S.H., Gancarz, I., Koberstein, J.T., 1988. Macromolecules 21: 2980
20. Broseta, D., Fredrickson, G.H., Helfand, E., Leibler, L., 1990. Macromolecules 23: 132
21. Müller, M., Binder, K., 1995. J.Chem.Soc.Faraday Trans. 91: 2369
22. Schubert, D.W., Stamm, M., 1996. Europhys.Lett., in press
23. Anastasiadis, S.H., Russell, T.P., Satija, S.K., Majkrzak, C.F., 1990. J. Chem. Phys. 92: 5677, and references therein
24. Fernandez, M.L., Higgins, J.S., Penfold, J., Ward, R.C., Shackleton, C., Walsh, D.J., 1988. Polymer 29: 1923.
25. Higashida, N., Kressler, J., Yukioka, S., Inoue. T., 1992. Macromolecules 25: 5259
26. Kressler, J., Higishida, N., Inoue, T., Heckmann, W., Seitz, F., 1993. Macromolecules 26: 2090.
27. Kressler, J., Zounek, A., Arai, E., Higishida, N., Sekimo, M., Inoue, T., to be published
28. Ellingson, P.C., Stand, D.A. Cohen, A., Sammler, R.L., Carriere, J., 1993. ACS/PMSE 69:183.
29. Semenov, A.N., 1994. Macromolecules 27: 2732; Semenov, A.N., to be published
30. Russell, T.P., Hjelm, R.P., Seeger, P.A. 1990. Macromolecules 23: 890.
31. Guckenbiehl, B., Stamm, M., Springer, T., 1994. Physica B 198: 127.
32. Guckenbiehl, B., Stamm, M., Springer, T., 1994.Colloids and Surfaces A86: 311.
33. Stamm, M., Hüttenbach, S., Reiter, G., Springer, T., 1991. Europhys. Lett. 14: 451.
34. Kunz, K., Stamm, M., 1994. Makromol. Chem., Macromol. Symp. 78: 105.
35. Kunz, K., Stamm, M., Harshorne, M., Affrossman, S., 1996. Acta Polymer. 47: 234.
36. Anastasiadis, S.H., Russell, T.P., Satija, S.H., Majkrzak, C.F., 1989. Phys.Rev.Lett. 62: 1852.
37. Anastasiadis, S.H., Russell, T.P., 1990. J.Chem.Phys. 92: 5677.
38. Menelle, A., Russell, T.P., Anastasiadis, S.H., Satija, S.H., Majkrzak, C.F., 1992. Phys.Rev.Lett. 68: 67.

(version 8.9.1996)